Appendix A. Supplementary data

Insight into the enhanced adsorption behavior and mechanism of ibuprofen from water on polyaniline/acid-impregnated reed biochar composite

Zhixian Zhou [1], Zhengxiang Li [1], Chenman Shi [1], Wenlong Zhang (✉)[1], Jiangtao Feng [3], Wei Yan[3], Hongjie Wang (✉)[1,2]

1 Hebei Key Laboratory of Close-to-Nature Restoration Technology of Wetlands, School of Eco-Environment, Hebei University, Baoding 071002, China

2 Engineering Research Center of Ecological Safety and Conservation in Beijing-Tianjin-Hebei (Xiong'an New Area) of MOE, Baoding 071002, China

3 Department of Environmental Science and Engineering, State Key Laboratory of Multiphase Flow in Power Engineering, School of Energy and Power Engineering, Xi'an Jiaotong University, Xi'an 710049, China

Contents

✉ Corresponding authors
E-mail: zhangwenlong@hbu.edu.cn (W. Zhang); wanghj@hbu.edu.cn (H. Wang)

Table S4 Estimated costs of industrial factors.

Texts:(S1-S4)

Text S1. Effect of calcination temperature.

Calcination process has been demonstrated to significantly impact the functional groups and structure of BC. It is evident from Fig. S1 that the adsorbents (H-BC and PANI/H-BC) calcined at 500°C both exhibited better adsorption performance than that at 400°C or 600°C. Furthermore, after loading with PANI, the adsorption capacity of the BC adsorbents was substantially improved. Before loading, H-BC-400 showed a higher adsorption capacity for IBP compared to H-BC-600. This phenomenon is likely attributed to the thermal decomposition reaction at elevated temperatures, which partially destroys the BC structure and hinders IBP adsorption(Zhang et al., 2024b). However, after modification, PANI/H-BC-600 exhibited better adsorption performance than that calcined at 400°C. This could be attributed to the formation of more amide groups through the condensation of abundant carboxylic acid groups with PANI at 600°C.

Text S2. IBP concentration test.

The concentration of IBP was measured by UV-VIS spectrophotometer（Persee TU1900, China）and calculated by standard curve method. The UV-Vis spectrophotometer was employed to measure the absorbance of IBP solutions with concentrations ranging from 0.1 to 10 mg/L at a wavelength of 224 nm and the standard curve for IBP was depicted in Fig. S2. The equation of the standard curve is $y = 16.648x - 0.0275$, with an R^2 value of 0.9996, indicating a strong linear relationship. This standard curve for IBP serves as a crucial basis for subsequent

single-factor experiments, adsorption kinetics studies, and isothermal adsorption experiments.

Text S3. Details of the adsorption experiment.

The adsorption performance of BC based adsorbents for IBP at 298K was evaluated through a series of adsorption tests. A standard solution containing 20 mg/L of IBP was prepared by dissolving 0.01 g of IBP in 50 mL of anhydrous ethanol in a 500 mL volumetric flask, and then diluting it to the mark with distilled water. Subsequently, the solution was utilized for batch analysis. Following the adsorption process, the filtrate was collected by a 5 mL syringe equipped with a 0.22 μm filter membrane after the addition of 2 g/L of adsorbent. The initial and equilibrium concentration were determined spectrophotometrically at a wavelength of 224 nm, employing a UV-VIS spectrophotometer (Persee TU1900, China).

The study investigated the impact of pH value on the adsorption performance, as outlined below. With the aid of HCl and NaOH, adjustments were made to the pH of the standard solution, varying it in steps of 1.0 from 3.0 up to 13.0. And in a 50 mL centrifuge tube, the adsorption process occurred by adding 20 mL of the standard solution along with 40 mg of adsorbent. Upon reaching adsorption equilibrium in a constant temperature oscillator at 200 r/min, the capacity for adsorbing IBP was calculated based on Eq. (S1). Also, the optimal pH value was selected for subsequent experiments.

The variation in the adsorption capacity of PANI/H-BC at different pH values (3, 7, and 11) with respect to the initial concentration of IBP (5, 10, 15, 20, 25, and 30

mg/L) was investigated. The adsorption process was conducted in 50 mL centrifuge tubes, with 20 mL of IBP solution at various concentrations and 40 mg of adsorbent added. The adsorption capacity was calculated after reaching adsorption equilibrium in a thermostatic shaker operating at 200 r/min.

The adsorption kinetics experiment involved contacting 200 mL of standard solution with 0.4 g of adsorbent in a 500 mL beaker. And the equilibrium was achieved through magnetic stirring at 200 r/min. The sampling intervals were 10 seconds, 30 seconds, 1 minute, 5 minutes, 10 minutes, 20 minutes, 30 minutes, 1 hour, 2 hours, 3 hours, 4 hours, and 5 hours. To study the kinetic adsorption mechanism, the pseudo-first-order kinetic model (Eq. (S2)) and the pseudo-second-order kinetic model (Eq. (S3)) were determined for modelling.

In general, 40 mg of adsorbents and 20 mL of IBP solution with varying concentrations are contacted in a 50 mL centrifuge tube for isothermal adsorption experiments. The concentrations of IBP solution are 2, 6, 8, 10, 14, 20, 24, and 30 mg/L, respectively. The isothermal adsorption experiment is conducted on a constant temperature oscillator rotating at 200 r/min until adsorption equilibrium is reached. Based on the experimental data, three different models were applied to describe the adsorption isotherm, namely Langmuir (Eq. (S4)), Freundlich (Eq. (S5)) and Temkin isotherm model (Eq. (S6)).

Text S4. Discussion on ecotoxicity.

To investigate the potential environmental impact of the adsorbent, the saturated PANI/H-BC was utilized for an acute toxicity experiment using photobacteria.

Specifically, 0.04 g of PANI/H-BC after saturated was mixed with 20 mL distilled water and oscillated at a constant temperature. Following sedimentation and filtration, the filtrate was collected as the leachate. The leachate was used for the acute toxicological test using Photobacterium phosphoreum, with a 3% NaCl solution serving as the control group. The luminescence inhibition rate of Photobacterium phosphoreum was measured after 15 minutes.

The test revealed a luminescence inhibition rate of 25% after 15 minutes of reaction, indicating that the material's leachate possesses low to moderate acute ecotoxicity, possibly attributable to the leaching of some acidic functional groups. Therefore, future research should focus on the potential toxicity or bioaccumulation of the material's leachate products. Besides, its long-term safety is further verified in conjunction with the actual environmental conditions.

Equations:(S1-S6)

$$Q_e = \frac{(C_0 - C_e)V}{m} \quad (1)$$

where Q_e (mg/g) is the IBP equilibrium adsorption capacity; C_0 and C_e (mg/L) indicate the initial and equilibrium concentration of IBP; V (L) was the initial volume of IBP solution; m (mg) is the mass of dry adsorbent.

$$\ln(Q_e - Q_t) = \ln Q_e - k_1 t \quad (2)$$

$$\frac{t}{Q_t} = \frac{1}{k_2 Q_e^2} + \frac{t}{Q_e} \quad (3)$$

where t (min) is the adsorption time and Q_t (mg/g) are the adsorption capacity at time t (min). k_1 (min^{-1}), k_2 (g/mg·min), are adsorption rate constant of pseudo-first order kinetic model and pseudo-second-order kinetic model.

$$Q_e = \frac{Q_m K_L C_e}{1 + K_L C_e} \quad (4)$$

$$Q_e = K_F C_e^{1/n} \quad (5)$$

$$Q_e = \frac{RT}{b} \ln C_e + \frac{RT}{b} \ln A \quad (6)$$

where Q_m (mg/g) and Q_e (mg/g) are the maximum adsorption capacity and equilibrium adsorption capacity, C_e (mg/g) is the concentration of equilibrium, K_L (L/mg) and K_F ($(mg^{(n-1)} \cdot L)^{1/n}/g$) are adsorption rate constant of Langmuir and

Freundlich models. 1/*n* related to the adsorption strength which is a dimensionless empirical parameter. *b* (kJ/mol) is related to the heat of sorption and A (L/g) is an equilibrium bond constant related to maximum bond energy. *T* (K) is the absolute temperature.

Tables:(S1-S4)

Table S1

The kinetic model parameters of IBP adsorbed by PANI/H-BC, PANI and H-BC.

Models	Parameters				
		Q_e^a (mg/g)	k_1/min^{-1}	Q_e^b (mg/g)	R^2
Pseudo-first-order	PANI/H-BC	8.5923	1.2092	8.0848	0.9116
	PANI	6.42	0.7843	6.2981	0.976
	H-BC	4.1935	5.62468	3.9301	0.889
		Q_e^a (mg/g)	k_2(g/mg·min)	Q_e^b (mg/g)	R^2
Pseudo-second-order	PANI/H-BC	8.5923	0.1944	8.3484	0.9726
	PANI	6.42	0.1729	6.5045	0.9782
	H-BC	4.1935	1.97328	4.0244	0.85381

Q_e^a is obtained from the experimental data. Q_e^b was calculated from the kinetics model

Table S2

The isotherm model parameters of IBP adsorbed by PANI/H-BC, PANI and H-BC.

Models	Parameters			
Langmuir model		Q_{max}(mg/g)	K_L(L/mg)	R^2
	PANI/H-BC	35.5758	0.04817	0.92256
	PANI	8.2391	0.0113	0.9900
	H-BC	9.4958	0.0829	0.9546
Freundlich model		$K_F((mg^{(n-1)} \cdot L)^{1/n}/g)$	*1/n*	R^2
	PANI/H-BC	1.7119	0.8469	0.9048
	PANI	0.5573	0.9836	0.9341
	H-BC	1.1374	0.5626	0.9787
Temkin model		*B*(kJ/mol)	A(L/g)	R^2
	PANI/H-BC	557.6349	1.0276	0.9045
	PANI	647.5112	3.8263	0.9881
	H-BC	2598.9426	7.4011	0.7498

Table S3

Comparison of cost estimation with other waste material.

Raw materials	Mode of preparation	Cost/kg (USD)	Reference
Synthetic zeolite from rice husk	Chemical treatment followed by pyrolysis	9.224	(Kyzas et al., 2015)
Kola nut husk	Carbonization and H_3PO_4	42.52	(Bello et al., 2021)
Sugarcane bagasse	Pyrolysis and H_3PO_4	3.81	(Chakraborty et al., 2018b)
	Pyrolysis and super-heated steam	3.49	
Orange peel	HTC and HNO_3	4.71	(Ngoc et al., 2023)
Teak sawdust	HTC and $ZnCl_2$	3.47	(Ngoc et al., 2023)
Teff straw	Pyrolysis and H_3PO_4	3.73	(Yihunu et al., 2019)
Rice husk	Zeolite	5.42	(Banerjee et al., 2017)
Reed	Pyrolysis and PANI loading	2.991	This work

Table S4

Estimated costs of industrial factors(Métivier-Pignon et al., 2003; Oladipo and Gazi, 2016; Samoraj et al., 2016).

Particulars	Sub sections	Cost analysis	Amount/ (USD)
Pretreatment	pH adjustment	unit[a]×per unit cost[b] $=0.8\times0.5\times10^{-3}$	0.0004
	Removal of suspended solids	unit×per unit cost $=1\times0.2\times10^{-3}$	0.0002
Equipment depreciation and maintenance	Reactor and Pipeline	invest×(1-rate[c])/ (year[d]×365×flow[e]) $=4\times10^{5}\times0.9/\ (10\times365\times10^{6})$	0.0001
	Adsorbent replacement	unit× per unit cost/flow $=100\times2.991/10^{6}$	0.001
	Maintain the filtration system	unit× per unit cost/flow $=10\times100/\ (30\times10^{6})$	0.00003
Prevent re-pollution	Disposal of residual chemicals	unit×per unit cost $=0.2\times0.3\times10^{-3}$	0.00006
Effluent quality	——	unit× per unit cost/flow $=1\times50/10^{6}$	0.00005
Total cost	——	——	0.00184

[a] unit: the quantity used.

[b] per unit cost: cost of electricity per kilowatt-hour.

[c]rate: residual value rate.

[d]year: depreciation year

[e]flow: the flow rate is calculated at 1000m³/d.

Figures:(S1-S9)

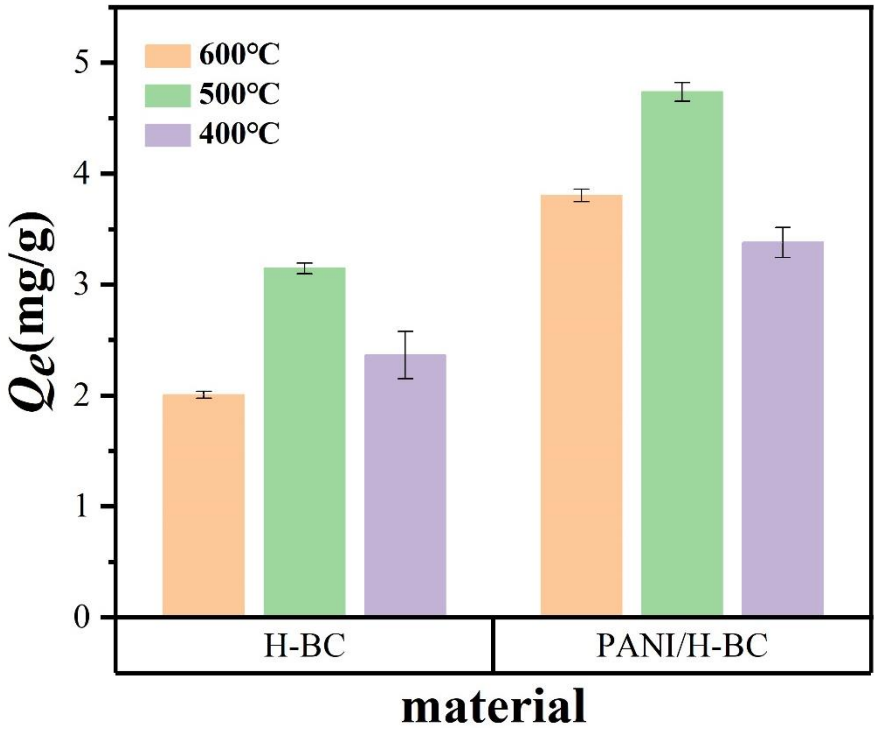

Fig. S1. Comparison of adsorption capacity of PANI/H-BC and H-BC for IBP at different calcination temperatures.

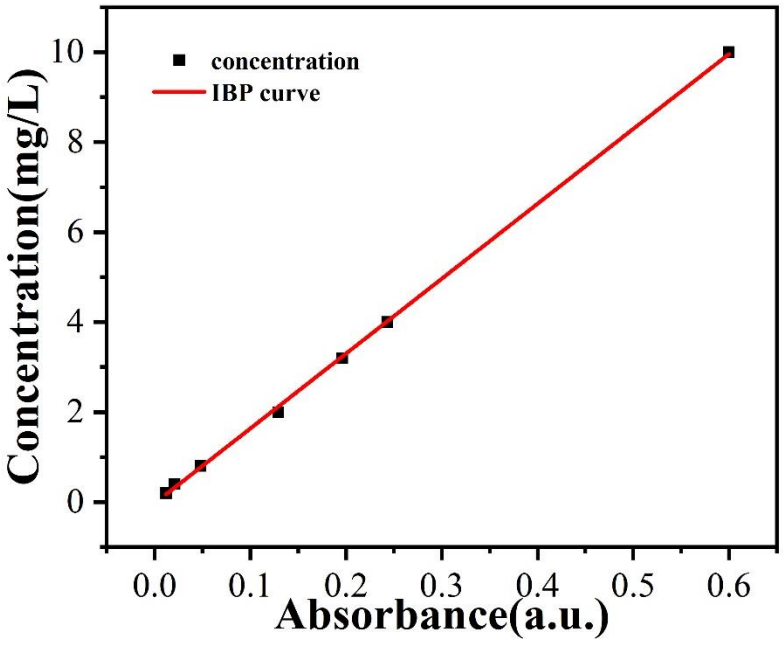

Fig. S2. IBP standard curve.

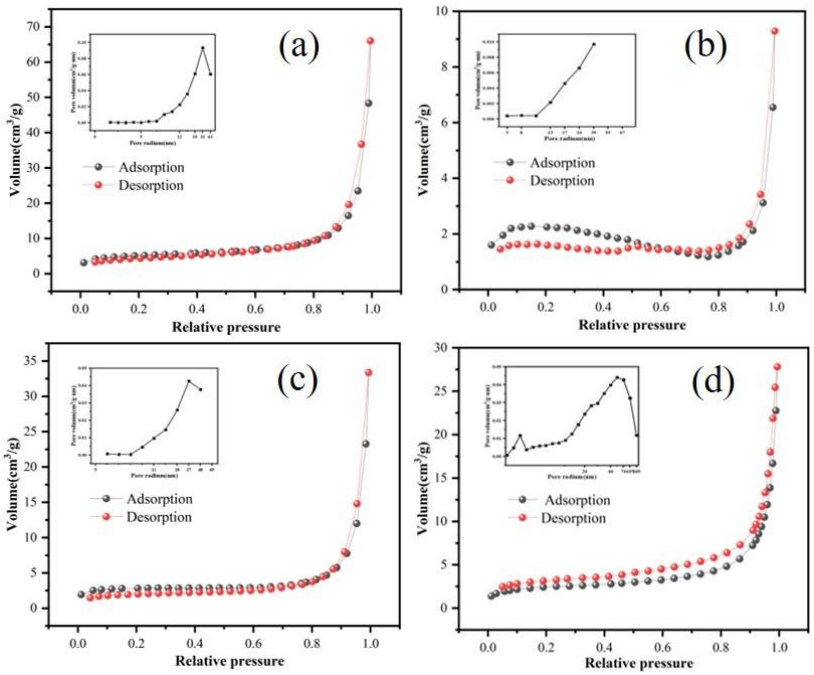

Fig. S3. N_2 gas adsorption-desorption isotherm and pore size distribution of (a) PANI, (b) H-BC, (c) PANI/H-BC before adsorption and (d) PANI/H-BC after desorption.

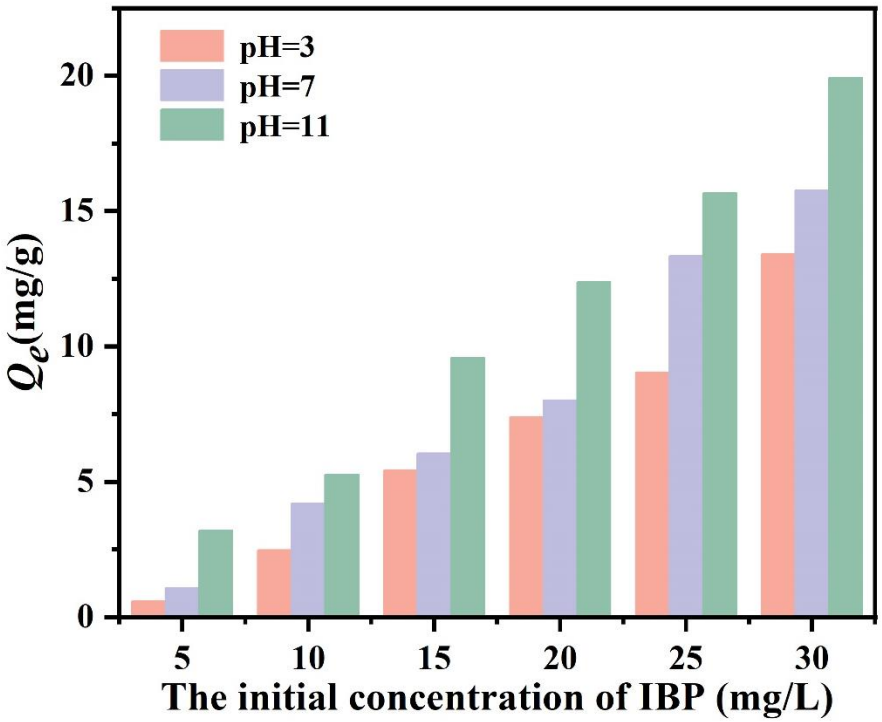

Fig. S4. The influence of pH and initial concentration on adsorption effect.

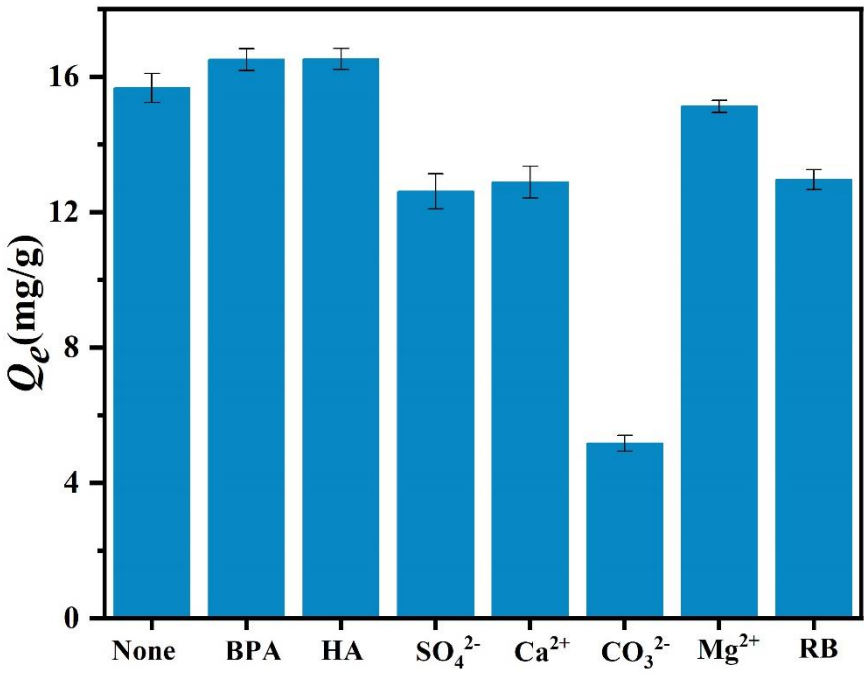

Fig. S5. The influence of different coexisting ions and organic substances on the adsorption of IBP on PANI/H-BC.

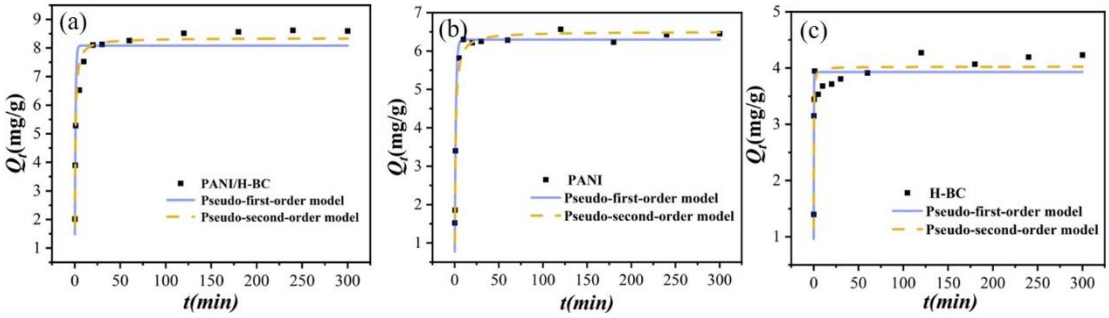

Fig. S6. Kinetic fitting curves of IBP adsorbed by (a) PANI/H-BC, (b) PANI and (c) H-BC.

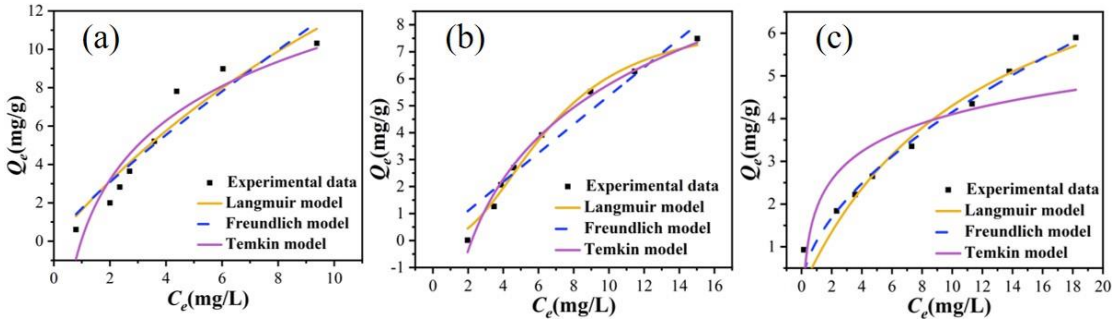

Fig. S7. The curve plots for the investigated isotherm models for (a) PANI/H-BC, (b) PANI and (c) H-BC adsorption.

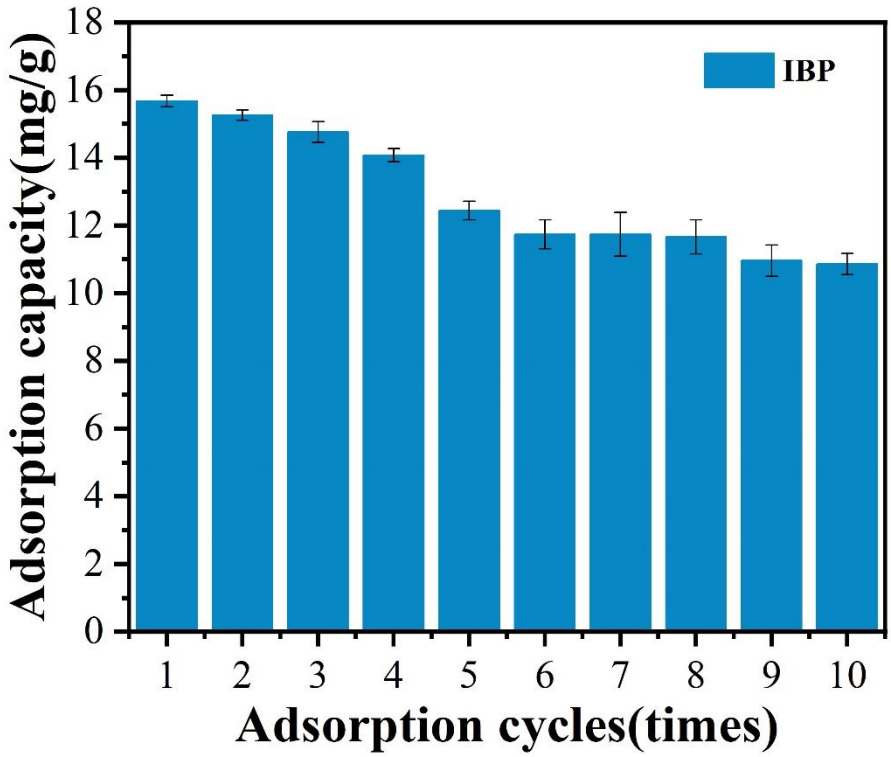

Fig. S8. The regenerability of IBP adsorption on PANI/H-BC using a mixed solution of ethanol and 0.01 mol/L NaCl.

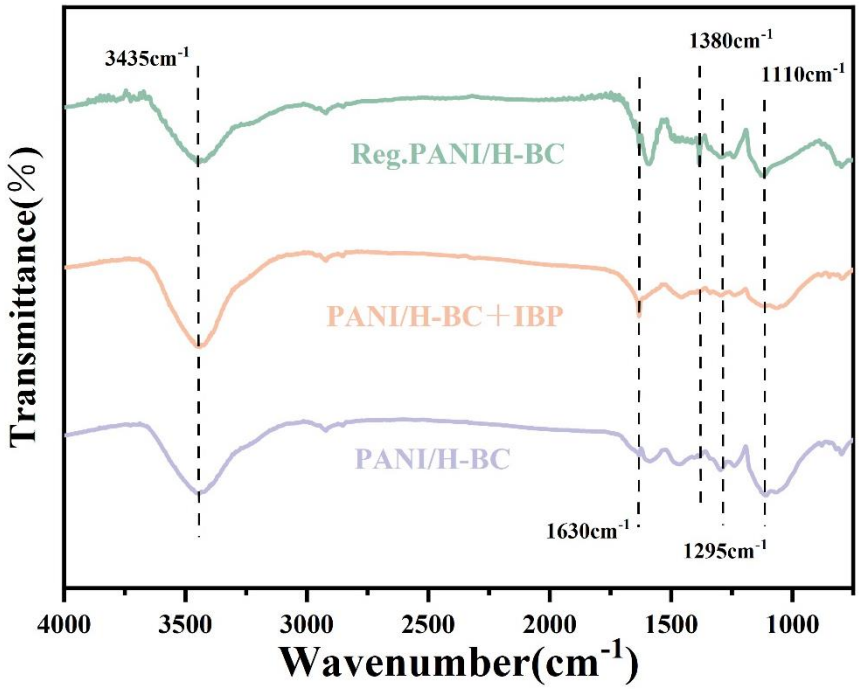

Fig. S9. FTIR spectra of PANI/H-BC before adsorption, after adsorption and after desorption.

References:

Banerjee S, Barman S, Halder G (2017). Sorptive elucidation of rice husk ash derived synthetic zeolite towards deionization of coalmine waste water: A comparative study. Groundwater for Sustainable Development, 5: 137-151

Bello O S, Alao O C, Alagbada T C, Agboola O S, Omotoba O T, Abikoye O R (2021). A renewable, sustainable and low-cost adsorbent for ibuprofen removal. Water Science and Technology, 83(1): 111-122

Chakraborty P, Show S, Banerjee S, Halder G (2018). Mechanistic insight into sorptive elimination of ibuprofen employing bi-directional activated biochar from sugarcane bagasse: Performance evaluation and cost estimation. Journal of Environmental Chemical Engineering, 6(4): 5287-5300

Kyzas G Z, Fu J, Lazaridis N K, Bikiaris D N, Matis K A (2015). New approaches on the removal of pharmaceuticals from wastewaters with adsorbent materials. Journal of Molecular Liquids, 209: 87-93

Métivier-Pignon H, Faur-Brasquet C, Jaouen P, Le Cloirec P (2003). Coupling ultrafiltration with an activated carbon cloth for the treatment of highly coloured wastewaters:: A techno-economic study. Environmental Technology, 24(6): 735-743

Ngoc D M, Hieu N C, Trung N H, Chien H H, Thi N Q, Hai N D, Chao H-P (2023). Tetracycline Removal from Water by Adsorption on Hydrochar and Hydrochar-Derived Activated Carbon: Performance, Mechanism, and Cost Calculation. Sustainability, 15(5): 4412

Oladipo A A, Gazi M (2016). Efficient boron abstraction using honeycomb-like porous magnetic hybrids: Assessment of techno-economic recovery of boric acid. Journal of Environmental Management, 183: 917-924

Samoraj M, Tuhy L, Rusek P, Rój E, Chojnacka K (2016). Pilot Plant Conversion of Blackcurrant Seeds into New Micronutrient Fertilizer Biocomponents via Biosorption. Bioresources, 11(1): 400-413

Yihunu E W, Minale M, Abebe S, Limin M (2019). Preparation, characterization and cost analysis of activated biochar and hydrochar derived from agricultural waste: a

comparative study. SN Applied Sciences, 1(8): 873

Zhang X, Hou J, Zhang S, Cai T, Liu S, Hu W, Zhang Q (2024). Standardization and micromechanistic study of tetracycline adsorption by biochar. Biochar, 6(1): 12